I&EC research
Industrial & Engineering Chemistry Research

Article

Cite This: Ind. Eng. Chem. Res. 2019, 58, 1417−1425

pubs.acs.org/IECR

Calcium Alginate Thin Films Derived from *Sargassum natans* for the Selective Adsorption of Cd^{2+}, Cu^{2+}, and Pb^{2+} Ions

Chantal Mohammed,[†] Shivanie Mahabir,[†] Kristy Mohammed,[†] Nigel John,[‡] Koon-Yang Lee,*[,+] and Keeran Ward*[,†]

[†]Department of Chemical Engineering and [‡]Department of Chemistry, The University of the West Indies St. Augustine, St. Augustine, Trinidad and Tobago

[+]Department of Aeronautics, Imperial College London, South Kensington Campus, SW7 2AZ London, United Kingdom

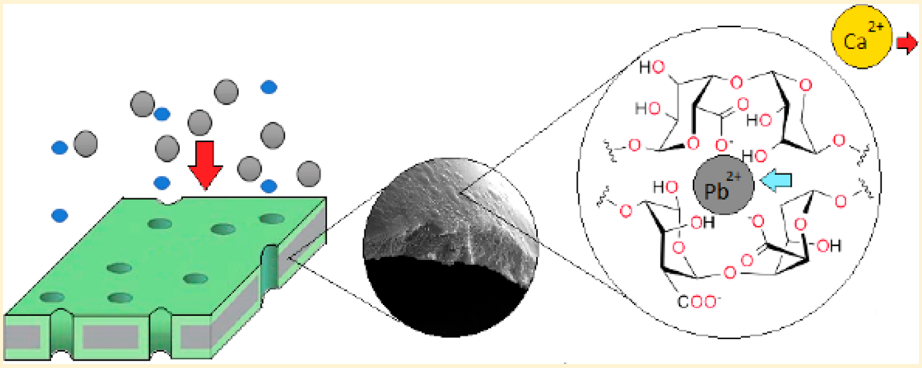

ABSTRACT: The Caribbean has seen the influx of *Sargassum*, affecting the livelihood of communities. Sodium alginate extracted from *Sargassum* is known for its cross-linking properties, making the seaweed attractive as an adsorbent. Hence, the use of calcium alginate thin films can decrease the mass transfer resistance found in commonly used alginate beads, resulting in increased adsorption efficiency. This Article discusses the potential of calcium alginate thin films for Pb^{2+}, Cu^{2+}, and Cd^{2+} ion adsorption. Pb^{2+}, Cu^{2+}, and Cd^{2+} adsorption fitted the Langmuir isotherm well with capacities of 0.80, 0.10, and 0.02 mmol of metal/g, respectively, for *Sargassum*. Kinetic studies showed that the ions followed the pseudo-second-order model, elucidating that ion exchange governed adsorption. Furthermore, NMR characterization showed that G-block monomers influenced kinetic parameters and selectivity in the following order: $Pb^{2+} > Cu^{2+} > Cd^{2+}$.

1. INTRODUCTION

Heavy metal ions such as Pb^{2+}, Cu^{2+}, and Cd^{2+}, even at low concentrations, pose serious sanitary and ecological concerns. Recently, industrial activities such as gasoline production have increased lead concentration, which affects the physiological processes of plants and increases the reaction of oxygen in species resulting in growth suppression.[1] Copper can enter the environment through activities such as mining, leading to negative effects on the gastrointestinal systems and vital organs such as the liver.[2] Cadmium has a high soil to plant transfer and as a result can be found in food, which results in damage to the kidney and bones.[3] The removal of these ions provides clean water, and these sequestered metals can be recovered for economical interest.[4,5] Therefore, a wide range of methods has been developed for the removal of heavy metals from solutions, including chemical precipitation,[6] ion exchange,[7] adsorption, cementation, and electrolysis.[8] These methods often involve chemicals, which may be energy intensive processes and, in some cases, ineffective at high concentrations.[9,10] The use of biomass as a potential adsorbent for the removal of these heavy metal ions could serve as an inexpensive and effective means of water treatment.[11]

Alginate, which can be extracted from the walls of brown seaweed, is a natural linear polysaccharide copolymer. It consists of two uronic acids: β-D-mannuronic acid (M) and α-L-guluronic acid (G).[12] The presence of these blocks in various ratios and molecular weight alters the physiochemical properties. The alginates that are rich in L-guluronate form strong but brittle gels, and those rich in D-mannuronate are weaker but more flexible.[13] These physiochemical properties vary depending on the type of seaweed and the geographical location. *Sargassum natans* (*S. natans*) is an invasive brown seaweed which has besieged Caribbean coastlines. *S. natans* has negatively impacted marine ecosystems resulting in a decrease in economic activities such as tourism and fishing.[14] Due to its abundance and invasive nature, there is an urgent need for its utilization as a possible beneficial raw material. Commercial alginates are usually extracted from brown seaweed such as kelps or *Laminariales*. These alginophytes are usually cultivated

Received: August 3, 2018
Revised: November 27, 2018
Accepted: December 26, 2018
Published: December 26, 2018

DOI: 10.1021/acs.iecr.8b03691
Ind. Eng. Chem. Res. 2019, 58, 1417−1425

for the production of alginates, while *S. natans* are in abundance naturally.[15]

Sodium alginate can be cross-linked with the addition of divalent ions, which leads to gelation due to the interaction between the carboxylate group and the divalent ion.[16] The most popular cross-linker is calcium, which is known to form the "egg box model". Calcium forms a permeable gel with a fast gelation rate.[17] In this model, the M and G blocks form a three-dimensional mesh which resembles the way in which eggs are held in an egg carton.[18] In the various junction zones of the egg box model, there exists an overall dimer shape that allows for the entrapment of ions/cells.[19] Alginates extracted from *S. natans* are known to have a low M:G ratio of approximately 0.47 and a high G-block content, resulting in a strongly cross-linked matrix and the formation of a stiff gel.[20,21] In addition to calcium ions, alginate also has a large affinity for divalent ions such as Pb^{2+}, Cu^{2+}, and Cd^{2+}, which increases with increasing G block content.[22] A study has shown that alginate is an electronegative host for divalent cations due to its ability to bind with the carboxylic group of the polyguluronic chain.[23] The interactions between the metal ion and the carboxylate group in the cross-linked alginate film resembles a unidentate coordination mode. However, there have been reports of bidentate chelating and bridging coordination.[23]

Nonliving biomass such as *Sargassum angostifolium* has been utilized for metal uptake, due to the different metal-adsorptive moieties present on or in the cell wall; these usually include the carboxylate and sulfonates group.[24,25] Both methods have exceptional adsorption properties for multiple metal ions. This concept has been utilized in past research, through the use of calcium alginate beads and brown seaweed biomass. These calcium alginate beads are made using extrusion dripping. A study done recorded the highest maximum adsorption capacity using pure calcium alginate beads from *Laminaria digitata* as 1.80, 1.79, and 1.53 mmol g^{-1} for Pb^{2+}, Cu^{2+}, and Cd^{2+}, respectively.[26] In an effort to optimize uptake, heavy metal ion gelation with alginate has also been explored and resulted in increased adsorption capacities of 2.10, 2.62, and 1.60 mmol g^{-1} for Pb^{2+}, Cu^{2+}, and Cd^{2+}.[27] This maximum adsorption capacity is dependent on the loading and the properties of the alginate as well as the type of biosorbent.[27] This has led to studies being carried out to increase the adsorption capacity by using different types of bioadsorbents such as composite beads and membranes.

Thin films have proven to be more attractive for heavy metal ion remediation than other forms of adsorbents. For instance, titanium dioxide (TiO_2) thin films exhibit greater efficiencies when compared to TiO_2 powders as ion exchange adsorbents due to its enhanced mass transfer properties.[28,29] As the film becomes thinner, there is an increase in diffusion across the film due to a decrease in the resistance to mass transfer according to Fick's second law.[30] Thin film coatings have also been used on inert materials for the adsorption of Pb^{2+} and compared to calcium alginate beads.[28] It was found that alginate coating had a higher binding capacity and attained equilibrium faster than the beads. The use of calcium alginate thin films from waste brown seaweed *S. natans* for heavy metal sorption has not been considered in past research and, hence, presents the novel contribution in the area of wastewater treatment. In this work, we report the potential of calcium alginate thin films derived from waste *S. natans* as an effective adsorptive surface for Pb^{2+}, Cu^{2+}, and Cd^{2+}.

2. MATERIALS AND METHODS

2.1. Materials. Alginate thin films were fabricated from sodium alginate purchased from Sigma-Aldrich (W201502, USA), Protanal GP 5450 and Manugel DMB (donated by FMC Biopolymer), and sodium alginate extracted from *S. natans*. Calcium chloride dihydrate (ACS reagent, purity ≥99%, Sigma-Aldrich) was used as the cross-linker. Atomic Absorption standard solutions (Analytik Jena, USA) for Pb^{2+}, Cu^{2+}, and Cd^{2+} were used for preparing standards and were tested using an Analytikjena novAA 300 spectrometer. Nuclear Magnetic Resonance (NMR) samples were prepared using hydrochloric acid (JT Baker, USA), NaOH (Rasayan Laboratory, USA), deuterium oxide (D_2O 99.9%), sodium deuteroxide (NaOD, 99%), and triethylenetetraminehexaacetic (TTHA) acid (≥98%) purchased from Sigma-Aldrich.

2.2. Fabrication of Calcium Alginate Thin Film. Sodium alginate solutions with a viscosity of 4000 cP were prepared by dissolving sodium alginate in deionized water at concentrations of 2.40% (w/v) for Protanal, 3.51% (w/v) for Manugel, 7.00% (w/v) for Sigma, and 9.33% (w/v) for *S. natans*, respectively, under constant stirring at 2000 rpm. The sodium alginate solution was then deaerated for 30 min using sonication prior to casting onto a glass sheet using a manual casting knife with a fixed height of 1 mm, followed by drying at 60 °C for 2 h until a thin sodium alginate film (<100 μm in thickness) was formed. The thin sodium alginate film was then cooled to room temperature prior to immersing into 3 L of 7% (w/v) $CaCl_2$ bath for 15 min. The calcium alginate film was then washed with deionized water, cut into discs of 3.5 cm in diameter using a surgical scalpel, and fixed onto Whatman Filter paper (Grade 1) as a support for subsequent use.

2.3. Investigation of the Adsorption Properties of Calcium Alginate Thin Films. *2.3.1. Adsorption Study.* The average thickness and mass of the calcium alginate thin films prior to each run were determined. Pb^{2+} solutions were prepared within the concentration range of 10−150 ppm, while solutions for Cu^{2+} and Cd^{2+} were prepared within the concentrations of 5−100 ppm. The pH was roughly 3.0 for all solutions. Batch experiments were carried out by pipetting 5 mL of each heavy metal concentration into 25 mL beakers and simultaneously inserting the calcium alginate films for 5 h at 22 °C. After the reaction time elapsed, the films were removed, and the remaining solution was diluted and analyzed using atomic absorption spectroscopy. All experimental runs were carried out in triplicates. The heavy metal uptake was determined using the following expression

$$q_e = (C_0 - C) \times \frac{V}{\mathrm{RMM} \times m} \quad (1)$$

where q_e (mmol/g) is the mass of metal ions adsorbed per unit volume of the thin film, and C_0 (mg/L) and C (mg/L) denote the initial and final concentration of the solution. m (g) is the mass of each film, and V (L) denotes the volume of the heavy metal ion solutions, respectively. RMM is the relative molecular mass (g/mol). A control experiment was carried out to quantify the specific adsorption of heavy metals by the Whatman filter paper support. It was found that the heavy metal uptake was negligible compared to the calcium alginate films for all heavy metal ions.

2.3.2. Isotherm Study. Langmuir isotherm can be used for adsorption onto a flat surface as long as Henry's Law holds

DOI: 10.1021/acs.iecr.8b03691
Ind. Eng. Chem. Res. 2019, 58, 1417−1425

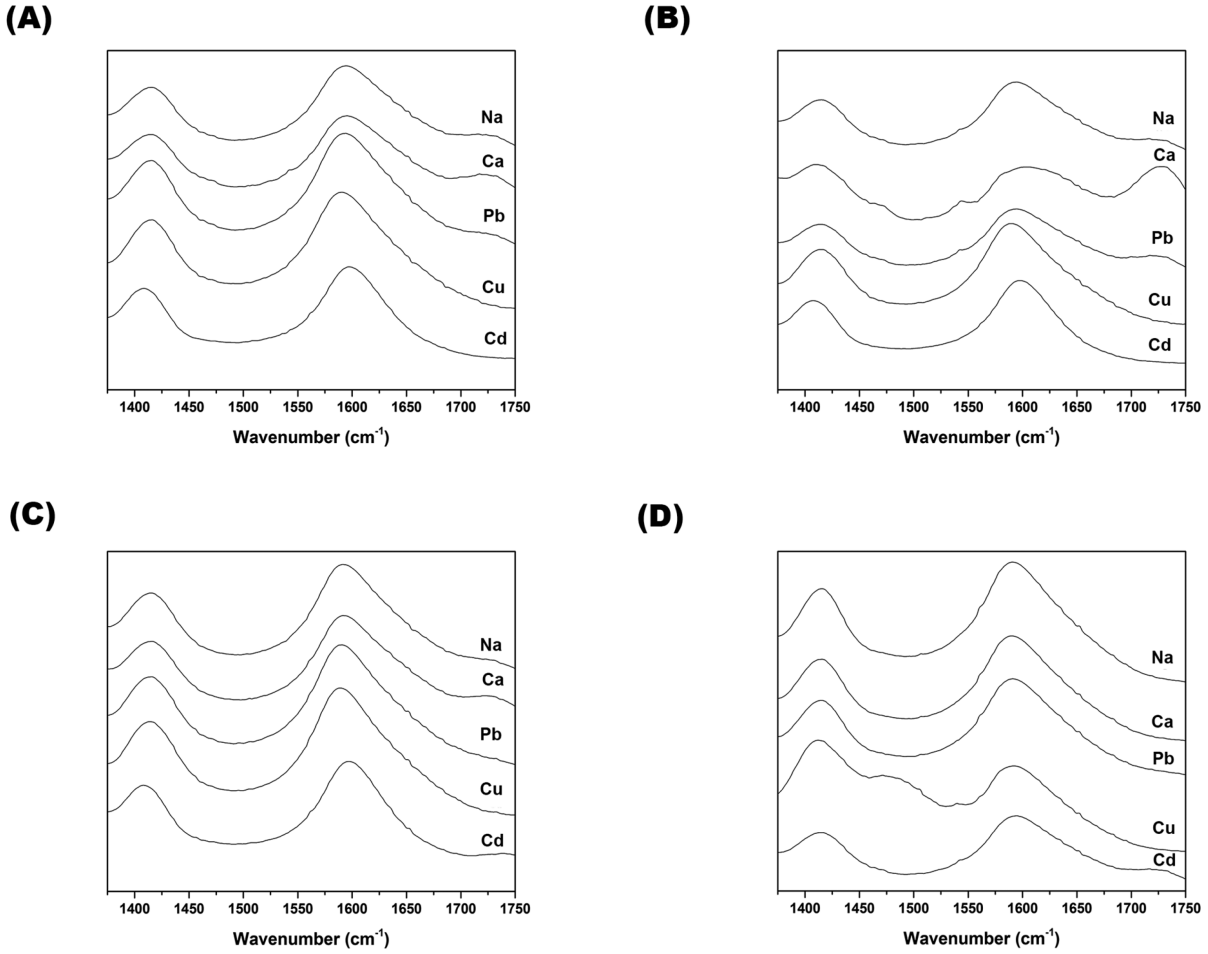

Figure 1. FTIR of Cd-, Cu-, Pb-, Ca-, and Na-alginate for (A) Manugel, (B) Protanal, (C) Sigma, and (D) *Sargassum* for wavenumber 1375 to 1700 cm^{-1}.

constant. The adsorption isotherm of various heavy metal ions by calcium alginate thin films was quantified using

$$q_e = \frac{q_{max} k_l C_e}{1 + k_l C_e} \quad (2)$$

where C_e is the equilibrium concentration remaining in solution (mmol L^{-1} of aqueous solution), q_{max} is the maximum monolayer capacity (mmol g^{-1}), and k_l is the equilibrium constant.[31] The Freundlich isotherm is a power law function, which can be applied to cases where there is adsorption onto energetically heterogeneous surfaces[32]

$$q_e = K_F C_e^{\frac{1}{n}} \quad (3)$$

where K_F is the Freundlich constant related to the amount of metal ions adsorbed, in the unit of (mmol g^{-1})(mmol L^{-1})$^{-1/n}$, and n is the sorption intensity.

2.3.3. Kinetic Study. Kinetic data was obtained using a similar procedure to the isotherm studies. This was done by varying the time taken (within 1−360 min) for a solution of 50 ppm Pb^{2+}, Cu^{2+}, and Cd^{2+} at 22 °C to be adsorbed. The pseudo-second-order model was used to determine the role of kinetics in the adsorption of ions by the film

$$q_t = \frac{k_2 q_e^2 t}{1 + k_2 q_e t} \quad (4)$$

where q_t is the metal concentration (mmol g^{-1}) at time t (min), q_e is the metal concentration (mmol g^{-1}) removed at equilibrium, and k_2 is the pseudo-second-order rate constant of sorption (g $mmol^{-1}$ min^{-1}).

The Weber Morris model was used to determine the mechanism involved in the adsorption of heavy metal ions onto calcium alginate films[33]

$$q_t = K_{id}\sqrt{t} \quad (5)$$

where K_{id} is the intraparticle diffusion rate (mmol g^{-1} $min^{-0.5}$). If the plot yields a straight line with a nonzero intercept, then intraparticle diffusion would not be the only rate-limiting step involved in the adsorption process.[34−36]

2.3.4. Selectivity Analysis. To quantify the selectivity of calcium alginate thin films, a mixed solution of 50 ppm Pb^{2+}, Cu^{2+}, and Cd^{2+} was first prepared. The respective calcium alginate thin film was then placed in the solution for 5 h, after which a sample was taken, diluted, and analyzed using atomic absorption spectroscopy. Selectivity was calculated according to the equation below

$$\text{Selectivity of } A = \frac{M_A}{M_A + M_B + M_C} \quad (6)$$

where M_i is the mass (mg) of component i adsorbed.

2.4. Characterization of the Calcium Alginate Film and Equilibrium Solution. *2.4.1. Fourier Transform*

DOI: 10.1021/acs.iecr.8b03691
Ind. Eng. Chem. Res. 2019, 58, 1417−1425

Table 1. $V_{asym}(COO^-)$, $V_{sym}(COO^-)$, and $\Delta V(COO^-)$ for Manugel, Protanal, Sigma, and *S. natans*

	Protanal			Manugel			Sigma			*S. natans*		
	V_{asym}	V_{sym}	ΔV	V_{asym}	V_{sym}	ΔV	V_{asym}	V_{sym}	ΔV	V_{asym}	V_{sym}	ΔV
Cd	1596	1421	191	1604	1420	184	1595	1422	173	1593	1420	173
Cu	1605	1418	187	1603	1422	181	1600	1418	182	1594	1416	178
Pb	1588	1420	168	1602	1418	184	1599	1418	181	1599	1416	183
Ca	1596	1418	178	1598	1417	181	1596	1419	177	1598	1417	181
Na	1603	1412	191	1602	1416	186	1603	1413	190	1611	1395	216

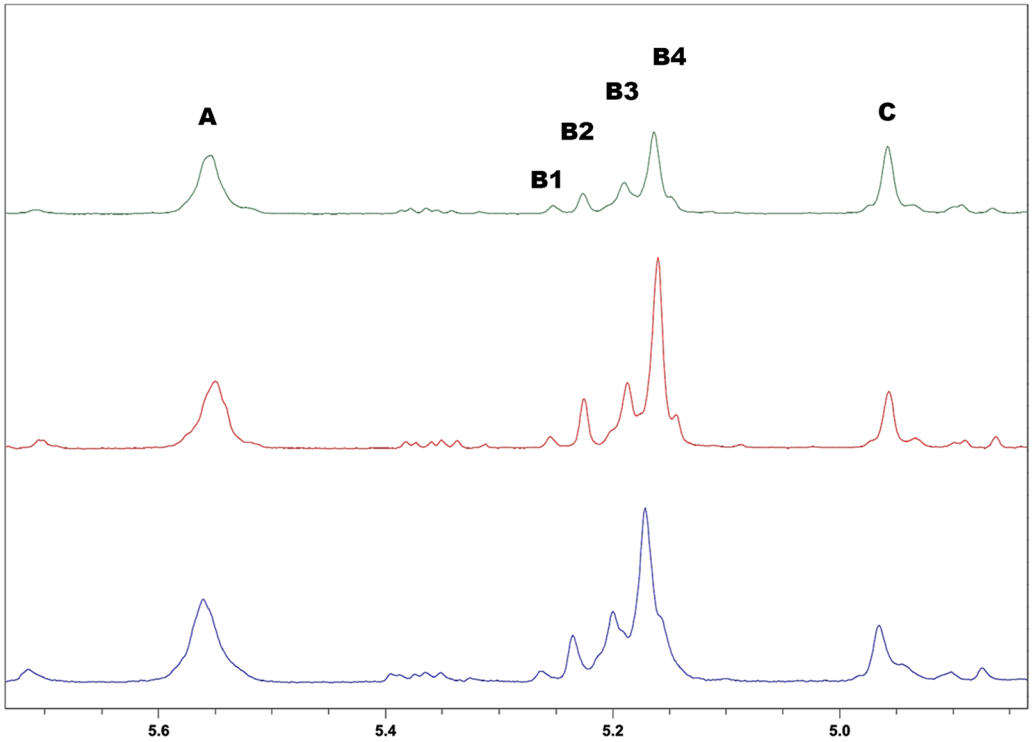

Figure 2. NMR characteristic peaks for Manugel, Sigma, and Protanal with peaks A (G), B1(GGM), B2(MGM), B3(MG), B4(MM), and C(GG).

Infrared Spectroscopy (FTIR). The spectra were recorded using a PerkinElmer Spectrum 400 FT-IR/FT-NIR spectrometer equipped with a universal ATR sampling accessory. The spectra were collected in the range of 650 to 4000 cm^{-1} with a resolution of 4 cm^{-1}. A total of 64 scans were used to obtain each spectrum.

2.4.2. Nuclear Magnetic Resonance (NMR). NMR analysis was done according to ASTM F2259-10 (2012). A 0.1% (w/v) sodium alginate solution was depolymerized using 0.1 M hydrochloric acid at a pH of 5.6. The solution was then heated for 1 h at 100 °C in a water bath. The pH was readjusted to 3.8 and placed into the water bath for a further 30 min. After this step, the pH was then adjusted to 7 by titrating the solution with a 0.1 M sodium hydroxide solution, followed by freeze-drying overnight. Approximately 10−12 mg of the freeze-dried sample was dissolved in 5 mL of D_2O. Prior to NMR, 0.7 mL of the alginate and 40 μL of 0.15 M TTHA were added to an NMR tube. H NMR spectra were obtained from a NMR Bruker AVANCE 600 MHz spectrometer operating at 80 °C and 20 Hz using a standard one-dimensional pulse program, a frequency of 600 MHz, a spectral window of 6 kHz with a 90° pulse angle, and an acquisition time of 5.453 s, collecting 65536 data points. 64 scans were accumulated for signal averaging. The chemical shifts of the anomeric proton signals were done according to the ASTM-F2259-10 method with A (guluronic acid anomeric proton), B1 (H-5 proton of the central guluronic acid residue in a GGM triad), B2 (H-5 proton of the central guluronic acid residue in a MGM triad), B3 (anomeric proton of the mannuronic acid residue neighboring a mannuronic acid), B4 (anomeric proton of the mannuronic acid residue neighboring a guluronic acid), and C (guluronic acid proton 5) at 5.2, 4.78, 4.75, 4.71, 4.68, and 4.48, respectively. The amount of G block and M block present is calculated using:

$$G = 0.5(A + C + 0.5(B1 + B2 + B3)) \quad (7)$$

$$M = B4 + 0.5(B1 + B2 + B3) \quad (8)$$

3. RESULTS AND DISCUSSION

3.1. Fourier Transform Infrared Spectroscopy (FTIR). FTIR analysis was carried out to identify the groups involved in the metal-alginate interaction for the commercial and extracted alginates (Figure 1). The wavenumber at 1600 cm^{-1} corresponds to the asymmetric stretching vibration (V_{asym} COO^-) of alginates, while the wavenumber at 1400 cm^{-1} corresponds to the symmetric vibration (V_{sym} COO^-). The asymmetric peak usually appears with a stronger intensity.[10,37]

Past studies have confirmed the existence of bidentate bridging coordination for the binding of sodium to the

DOI: 10.1021/acs.iecr.8b03691
Ind. Eng. Chem. Res. 2019, 58, 1417−1425

carboxylate group (free or available carboxylate ion). Models have proposed that the electronegative cavity (binding site) is created by a pair of guluronic acids. Within this structure, the oxygen atoms are involved in the coordination of the metal ion.[38] The nature of the ligand−metal interaction is highly sensitive to the type of coordination which occurs. Past studies have indicated that a relationship exists between the differences in the frequencies of the asymmetric and symmetric peaks [$\Delta V = V(COO^-)_{asym} - V(COO^-)_{sym}$] with respect to the free carboxylate ion, giving insight into the type of coordination occurring:[23]

Bidentate chelating: $\Delta V(COO^-)_{complex} << \Delta V(COO^-)_{Na}$

Bidentate bridging: $\Delta V(COO^-)_{complex} \approx \Delta V(COO^-)_{Na}$

Unidentate: $\Delta V(COO^-)_{complex} >> \Delta V(COO^-)_{Na}$

From Table 1, it can be seen that ΔV determined for the metal-alginate films fabricated from all brands differs from its free carboxylate by an insignificant value (i.e., <200 cm^{-1}). This infers that the metal−ligand interaction results in similar coordination to its sodium-ligand interactions, and thus it can be postulated that bidentate bridging coordination occurs.[23]

3.2. Nuclear Magnetic Resonance (NMR). Alginate consists of β-D-mannuronate (M) and C-5 epimer α-L-guluronate (G) linked by (1 → 4) glycoside bonds. By understanding parameters such as the M:G ratio and the amount of guluronic acid present (F_G), the potential and purpose of the alginate become clearer. The commercial sodium alginate brands were found to have similar chemical shifts (Figure 2). These chemical shifts were also similar to those found for alginate extracted from *S. natans*.[39] M:G ratios were calculated from eqs 7 and 8 and are shown in Table 2.

Table 2. Uronic Acid Compositions and the M:G Ratio for Alginates Types Used[a]

	F_G	F_M	M:G	ref
Manugel	0.56	0.44	0.79	this study
			0.71	41
Protanal	0.37	0.63	1.71	this study
			1.86	57
Sigma	0.44	0.56	1.29	this study
			1.60	58
S. natans	0.66	0.34	0.51	39

[a] $F_G = G/(M+G)$, $F_M = M/(M+G)$, and $M/G = (1-F_G)/F_G$.

Alginates that have low M:G ratios are expected to form strong but brittle gels and can therefore be used for environmental, biomedical, bioremediation, and encapsulation purposes due to its high G-content.[40] Alginate extracted from *S. natans* has a high G-block content and therefore is expected to have a high propensity for heavy metal ions. When cross-linked with divalent ions, the existence of M−blocks affects the gel formed due to cooperative binding.[41] Past studies have shown that elastic gels are formed when GG < MM < MG, and stiff gels are formed when MG < MM < GG.[20] It can be elucidated that sodium alginate extracted from *S. natans* will form a stiff gel, resulting in the formation of a strong film with a high selectivity for heavy metal ions.

3.3. Adsorption Characteristics. Figure 3 summarizes the concentration of heavy metal ions (Pb^{2+}, Cu^{2+}, and Cd^{2+}) adsorbed by the calcium alginate thin films as a function of concentration remaining in solution. It can be seen that the concentration adsorbed increases with increasing the remaining concentration. The Langmuir and Freundlich isotherms are typically used to model adsorption processes. The nonlinear plots reflect a Langmuir type adsorption process; that is a steady increase, until a saturation point is reached. In addition, the Langmuir plots resulted in higher linear regressions (R^2 > 0.95) than the Freundlich isotherm (R^2 < 0.95); therefore, the Langmuir model was used as a suitable fit for the adsorption process.

S. natans has the highest G-blocks concentration (F_G) and the lowest M:G ratio as shown in Table 2, thus having the largest amount of preferred binding sites. The converse is true for Protanal. Using the linearized Langmuir model (eq 3), *S. natans* had the highest maximum monolayer adsorption for Pb^{2+}, followed by Sigma, Manugel, and Protanal (see Table 3). At the saturation point, the film has reached its maximum capacity regardless of the free ions available for adsorption.

A similar trend is observed for Cu^{2+} but not Cd^{2+}, which had the lowest adsorption capacity for *S. natans*. This can be explained by looking at the M-block concentrations (F_M) shown in Table 2. Previous studies done have shown that an increase in the M:G ratio results in increased Cd^{2+} adsorption capacity, but an increase in the G-block concentration had no effect. This is due to the similarity in ionic radius of calcium and cadmium, which is critical for steric placement, and the rigidity of the GG linkage.[11] This gives cadmium an ability to distinguish between binding sites, and thus a preferential binding to the M-block can be expected.[26]

In the comparison of the maximum adsorption capacities in Table 3, it can be seen that Pb^{2+} has the highest capacity followed by Cu^{2+} and Cd^{2+}. The electronegativity, ionization energy, and acidity of Pb^{2+}, Cu^{2+}, and Cd^{2+} are summarized in Table 4. Pb^{2+} has the lowest ionization energy which implies that the enthalpy associated with the ion exchange reaction is low.[42] Furthermore, Pb^{2+} has the highest electronegativity, which is an indication of the ease for which charges can travel within solution, thus allowing for binding and the formation of metal-alginates. Hence, Pb^{2+} corresponds to the highest adsorption capacity due to its ability to take part in ion exchange/adsorption.[26,43] This explanation also corroborates with the results shown with Cu^{2+} and Cd^{2+}. Furthermore, the hard−soft-acid−base theory can be used to validate the metal affinity. This theory states that hard acids preferentially bind with hard bases and soft acids preferentially bind with soft bases. Pb^{2+} and Cu^{2+} are categorized as intermediate acids and Cd^{2+} as a soft acid. Thus, Pb^{2+} and Cu^{2+} bind more readily to the carboxyl group which is considered a "hard" base.[26,44] Hence, the strength of metal binding based on the acidity and electronegativity is as follows: $Pb^{2+} > Cu^{2+} > Cd^{2+}$.[45]

The selectivity of a metal ion is an indicator of the strength of binding of the heavy metal ion to a surface, by displacing lighter ions (K^+, Ca^{2+}, Mg^{2+}). From Figure 4, it can be seen that the selectivity of heavy metal ions follows the trend of $Pb^{2+} > Cu^{2+} > Cd^{2+}$ regardless of the type of alginate used. This selectivity is directly related to the affinity of the metal ions.[42,46] The increased adsorption capacity increases with increasing affinity, thus a greater bond strength is obtained, providing more stable metal-alginate complexes.[47] Films produced from *S. natans* have the highest selectivity for Pb^{2+} and the second highest selectivity for Cu^{2+} and Cd^{2+}. Furthermore, by comparing the adsorption performance (Table 3), it can be inferred that films fabricated from *S.*

DOI: 10.1021/acs.iecr.8b03691
Ind. Eng. Chem. Res. 2019, 58, 1417−1425

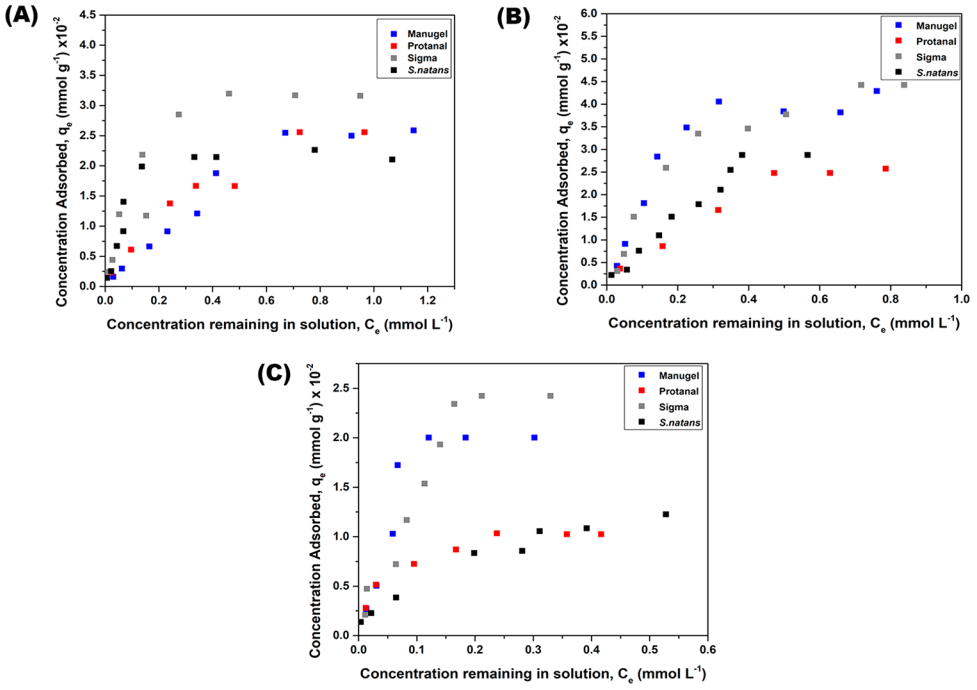

Figure 3. The adsorption characteristics of all brands of sodium alginate for (A) Pb^{2+} (B) Cu^{2+}, and (C) Cd^{2+} ions.

Table 3. Mean Parameter Data for Cu^{2+}, Cd^{2+}, and Pb^{2+} Adsorption[a]

		Langmuir isotherm			Freundlich isotherm		
ion	brand	R^2	max. adsorption, $q_{max} \times 10^{-2}$ (mmol g^{-1})	dissociation constant	R^2	Freundlich capacity, $K_F \times 10^{-2}$ (mmol g^{-1})(mmol L^{-1})$^{-1/n}$	intensity, n
Pb^{2+}	Manugel	0.99	13.8	0.65	0.97	6.05	1.21
	Protanal	0.98	8.8	1.69	0.95	6.32	1.21
	Sigma	0.98	12.7	2.30	0.84	8.71	1.96
	S. natans	0.99	79.8	0.32	0.79	8.55	1.73
Cu^{2+}	Manugel	0.97	7.5	2.84	0.81	1.03	1.81
	Protanal	0.96	5.6	1.19	0.92	3.51	1.42
	Sigma	0.96	7.4	2.12	0.94	6.35	1.42
	S. natans	0.96	10.1	0.89	0.98	6.44	1.11
Cd^{2+}	Manugel	0.95	3.2	15.06	0.63	7.81	1.94
	Protanal	0.98	2.4	24.36	0.96	3.51	3.48
	Sigma	0.99	4.2	19.17	0.85	9.00	1.86
	S. natans	0.98	1.9	61.94	0.93	2.89	2.54

[a]Coefficient of variance measured was <5%.

Table 4. Properties of Pb^{2+}, Cu^{2+}, and Cd^{2+} Ions[42]

metal	electronegativity (Pauling's)	ionization energy (kJ/mol)	acidity
Pb^{2+}	2.33	1450	intermediate
Cu^{2+}	1.9	1957	intermediate
Cd^{2+}	1.7	1631	soft

natans follow similar trends in metal affinity as the commercial alginates, with high adsorption capacities. This highlights the potential of *S. natans*, an invasive and waste brown seaweed, as an adsorbent for these heavy metal ions.

3.4. Kinetic Studies. The use of kinetic models can be applied to predict the binding mechanism involved in the sorption process, as well as insight into the adsorption rate.[48,49] Typically, models used are the pseudo-first-order and pseudo-second-order along with the Weber Morris model. The pseudo-first-order typically holds for boundary layer diffusion,

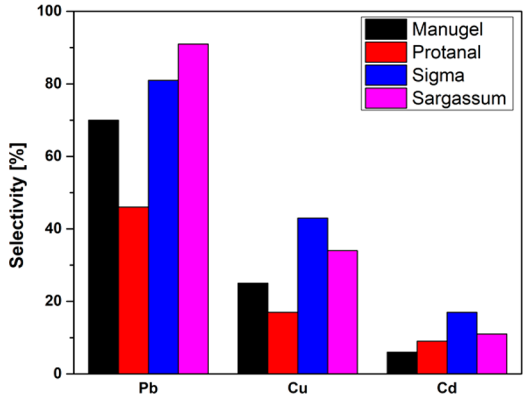

Figure 4. Selectivity of Pb^{2+}, Cu^{2+}, and Cd^{2+} with varying alginate brands.

DOI: 10.1021/acs.iecr.8b03691
Ind. Eng. Chem. Res. 2019, 58, 1417−1425

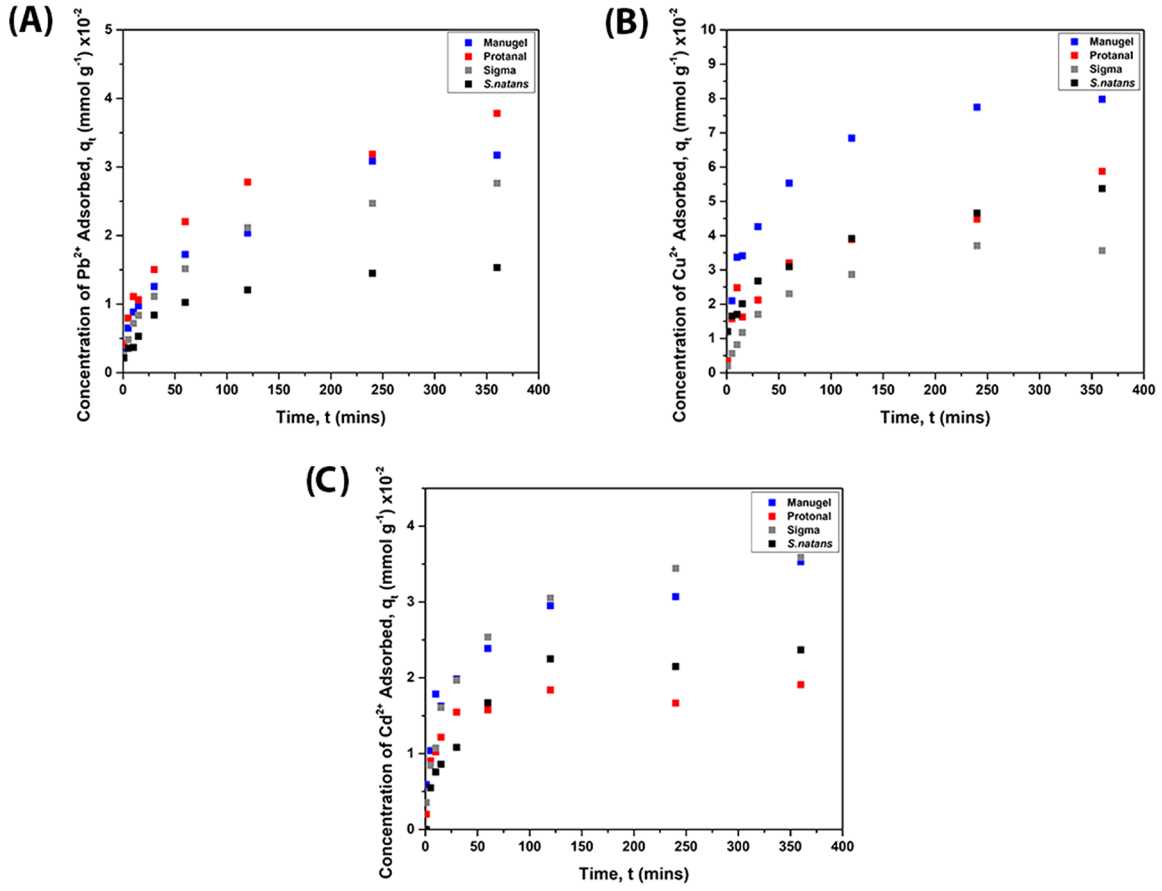

Figure 5. Concentration adsorbed against time for (A) Pb^{2+}, (B) Cu^{2+}, and (C) Cd^{2+} ions.

Table 5. Mean Parameter Data for Kinetic Models for Cu^{2+}, Cd^{2+}, and Pb^{2+}[a]

		pseudo-second-order			Weber Morris model	
ion	brand	equilibrium capacity, q_e, (mmol g^{-1}) $\times 10^{-2}$	rate constant, k_2, (g $mmol^{-1}$ min^{-1}) $\times 10^{-1}$	R^2	diffusion rate, k_{id}, (mmol g^{-1} $min^{-1/2}$) $\times 10^{-3}$	R^2
Pb^{2+}	Manugel	3.42	7.65	0.97	1.63	0.98
	Protanal	3.90	7.64	0.98	1.84	0.97
	Sigma	2.93	9.50	0.99	1.42	0.97
	S. natans	1.61	23.27	0.99	0.76	0.93
Cu^{2+}	Manugel	8.44	51.01	1.00	3.93	0.88
	Protanal	5.84	48.77	0.96	2.61	0.93
	Sigma	3.96	73.87	0.99	2.00	0.93
	S. natans	5.45	70.71	0.98	2.31	0.99
Cd^{2+}	Manugel	3.53	160.82	0.99	1.46	0.89
	Protanal	1.88	611.20	0.99	0.70	0.65
	Sigma	3.76	121.47	1.00	1.78	0.90
	S. natans	2.50	149.76	0.99	1.25	0.86

[a]Coefficient of variance measured was <5%.

while the pseudo-second-order holds for reactions and electrostatic forces.[5] Hence, if adsorption is governed by ion exchange, the pseudo-second-order fit can aid in explaining the phenomena. Kinetic studies previously conducted have shown that the pseudo-second-order was found to fit the adsorption of divalent metal ions and the release of calcium ions from an alginate surface.[42,50] A pseudo-second-order fit implies that a chemisorption process occurs.[51] During ion exchange between metal ions and the calcium alginate film, chemisorption occurs as the calcium ion is released and the metal ion is adsorbed. The chemisorption site occurs where the covalent bonding between the carboxyl groups creates sites for metal ion sharing or exchange.[52]

From Figure 5, it can be seen that the concentration adsorbed increases rapidly at the start of the experiment and then decreases, until the film becomes saturated. In this study, the linearized pseudo-second-order (eq 5) fits the adsorption process for all types of alginates as shown in Table 5 (R^2 > 0.95), and hence it can therefore be deduced that ion exchange governs the binding mechanism.

Fick's law implies that a decrease in thickness and a large interfacial area can enhance diffusion across a barrier.[53] Thin

DOI: 10.1021/acs.iecr.8b03691
Ind. Eng. Chem. Res. 2019, 58, 1417−1425

films have been known to support a faster rate of removal of ions and hence a larger adsorption capacity.[49] Of all the calcium alginate films investigated, Protanal was the thinnest (0.037 mm), followed by Manugel (0.068 mm), Sigma (0.100 mm), and *S. natans* (0.131 mm). This variation in thickness was as a result of varying initial sodium alginate concentrations in water. Therefore, as shown in Table 5, Protanal was observed to give high equilibrium adsorption capacities of 3.90 and 5.84 × 10^{-2} mmol g^{-1} for Pb^{2+} and Cu^{2+}, respectively. Conversely, *S. natans*, which had the thickest film, resulted in low equilibrium adsorption capacities. An increase in the kinetic rate constants as the alginate increases in concentration is observed due to the increase in G-blocks. *S. natans* has the highest G-block concentration which results in ions moving quickly to the binding sites.[53] This results in rapid saturation from the outside to the inside. This fact coupled with the film thickness leads to a low overall uptake and a low equilibrium adsorption capacity.[5] However, this large kinetic rate due to the increased G-block concentration results in a high monolayer adsorption capacity as shown in Table 3.[54]

The linear fit of the Weber Morris model (eq 6) as shown in Table 5 signifies that diffusion was involved in the biosorption process but it was not the rate controlling step.[36,55] The diffusion rate is dependent on thickness, and thus it can be observed that Protanal has the highest diffusion rate.[53] Surface adsorption can explain the low R^2 (see Table 5) values reported which places the rate-determining step as external film diffusion.[35,56] The external diffusion of Cd^{2+} to the surface of the film is dependent on the sites available for binding and thus increases with increasing M-block concentration. Thus, Pb^{2+} has the highest diffusion rates, followed by Cu^{2+} and Cd^{2+}.

4. CONCLUSION

This paper investigates the adsorption potential of calcium alginate thin films derived from *Sargassum natans*. It was found that the adsorption process followed the Langmuir isotherm for Pb^{2+}, Cu^{2+}, and Cd^{2+}, with a high adsorption capacity and selectivity in the following order: Pb^{2+} > Cu^{2+} > Cd^{2+}. Films produced from *S. natans* gave high kinetic rates due to increased G-block concentration resulting in low equilibrium adsorption capacities. Furthermore, rate kinetics followed the pseudo-second-order model suggesting that adsorption was strongly governed by ion exchange, with diffusion and binding coordination playing a major role. The results of this study provide insight into applying calcium alginate thin films from *S. natans* as a successful biosorbent for the adsorption of heavy metal ions.

AUTHOR INFORMATION

Corresponding Authors

*Phone: +1 868 730 1930. E-mail: keeran.ward@sta.uwi.edu (K.W.).

*Phone: +44 (0)20 7594 5150. E-mail: koonyang.lee@imperial.ac.uk (K.Y.L.).

ORCID

Koon-Yang Lee: 0000-0003-0777-2292

Notes

The authors declare no competing financial interest.

ACKNOWLEDGMENTS

This contribution was invited for submission following the presentation by Koon-Yang Lee that was identified by Session Chair Maren Roman, Virginia Tech, USA as the Best Presentation in the "New Horizons in Sustainable Materials" session of the 2018 ACS Spring National Meeting in New Orleans. The authors would like to thank Larry Bachansingh, Bissoon Parasram, Pooran Chaitram, Meera Bissram, and Andrew Pounder. We would also like to extend our gratitude to FMC Biopolymer and Department of Chemistry at the University of the West Indies.

REFERENCES

(1) Najeeb, U.; Ahmad, W.; Zia, M. H.; Zaffar, M.; Zhou, W. Enhancing the lead phytostabilization in wetland plant Juncus effusus L. through somaclonal manipulation and EDTA enrichment. *Arabian J. Chem.* **2017**, *10*, S3310−S3317.

(2) N. R. C. *Copper in Drinking Water*; National Academies Press: United States, 2000; DOI: 10.17226/9782.

(3) Satarug, S.; Garrett, S. H.; Sens, M. A.; Sens, D. A. Cadmium, Environmental Exposure, and Health Outcomes. *Environ. Health Perspect.* **2010**, *118*, 182−190.

(4) Pandey, A.; Bera, D.; Shukla, A.; Ray, L. Studies on Cr(VI), Pb(II) and Cu(II) adsorption-desorption using calcium alginate as biopolymer. *Chem. Speciation Bioavailability* **2007**, *19*, 17−24.

(5) Mata, Y. N.; Blázquez, M. L.; Ballester, A.; González, F.; Muñoz, J. A. Biosorption of cadmium, lead and copper with calcium alginate xerogels and immobilized Fucus vesiculosus. *J. Hazard. Mater.* **2009**, *163*, 555−562.

(6) Ku, Y.; Jung, I.-L. Photocatalytic reduction of Cr(VI) in aqueous solutions by UV irradiation with the presence of titanium dioxide. *Water Res.* **2001**, *35*, 135−142.

(7) Hamdaoui, O. Removal of copper(II) from aqueous phase by Purolite C100-MB cation exchange resin in fixed bed columns: Modeling. *J. Hazard. Mater.* **2009**, *161*, 737−746.

(8) Shim, H. Y.; Lee, K. S.; Lee, D. S.; Jeon, D. S.; Park, M. S.; Shin, J. S.; Lee, Y. K.; Goo, J. W.; Kim, S. B.; Chung, D. Y. Application of Electrocoagulation and Electrolysis on the Precipitation of Heavy Metals and Particulate Solids in Washwater from the Soil Washing. *J. Agric. Chem. Environ.* **2014**, *3*, 130−138.

(9) Cheremisinoff, N. P. *Handbook of Water and Wastewater Treatment Technologies*; Butterworth-Heinemann: Woburn, 2002.

(10) Volesky, B.; Holan, Z. R. Biosorption of heavy metals. *Biotechnol. Prog.* **1995**, *11*, 235−250.

(11) Davis, T. A.; Llanes, F.; Volesky, B.; Mucci, A. Metal Selectivity of Sargassum spp. and Their Alginates in Relation to Their α-l-Guluronic Acid Content and Conformation. *Environ. Sci. Technol.* **2003**, *37*, 261−267.

(12) Murguía-Flores, D. A.; Bonilla-Ríos, J.; Canales-Fiscal, M. R.; Sánchez-Fernández, A. Protein adsorption through Chitosan−Alginate membranes for potential applications. *Chem. Cent. J.* **2016**, *10*, 26.

(13) Toti, U. S.; Aminabhavi, T. M. Different viscosity grade sodium alginate and modified sodium alginate membranes in pervaporation separation of water + acetic acid and water + isopropanol mixtures. *J. Membr. Sci.* **2004**, *228*, 199−208.

(14) Louime, C.; Fortune, J.; Gervais, G. Sargassum Invasion of Coastal Environments: A Growing Concern. *Am. J. Environ. Sci.* **2017**, *13*, 58−64.

(15) Peteiro, C. Alginate Production from Marine Macroalgae, with Emphasis on Kelp Farming. *Springer Ser. Biomater. Sci. Eng.* **2018**, *11*, 27−66.

(16) Simpliciano, C.; Clark, L.; Asi, B.; Chu, N.; Mercado, M.; Diaz, S.; Goedert, M.; Mobed-Miremadi, M. Cross-Linked Alginate Film Pore Size Determination Using Atomic Force Microscopy and Validation Using Diffusivity Determinations. *J. Surf. Eng. Mater. Adv. Technol.* **2013**, *3*, 1−12.

DOI: 10.1021/acs.iecr.8b03691
Ind. Eng. Chem. Res. 2019, 58, 1417−1425

(17) Kuo, C.; Ma, P. Ionically Crosslinked Alginate Hydrogels As Scaffolds for Tissue Engineering: Part 1. Structure, Gelation Rate and Mechanical Properties. *Biomaterials* **2001**, *22*, 511−21.
(18) Russo, R.; Malinconico, M.; Santagata, G. Effect of Cross-Linking with Calcium Ions on the Physical Properties of Alginate Films. *Biomacromolecules* **2007**, *8*, 3193−7.
(19) Li, L.; Fang, Y.; Vreeker, R.; Appelqvist, I.; Mendes, E. Reexamining the Egg-Box Model in Calcium−Alginate Gels with X-ray Diffraction. *Biomacromolecules* **2007**, *8*, 464−468.
(20) Draget, K. I.; Smidsrød, O.; Skjåk-Bræk, G. *Food Polysaccharidesand Their Applications*; CRC Press-Taylor & Francis Group: United States, 2006.
(21) Rhein-Knudsen, N.; Ale, M. T.; Ajalloueian, F.; Meyer, A. S. Characterization of alginates from Ghanaian brown seaweeds: Sargassum spp. and Padina spp. *Food Hydrocolloids* **2017**, *71*, 236−244.
(22) Davis, T. A.; Volesky, B.; Mucci, A. A review of the biochemistry of heavy metal biosorption by brown algae. *Water Res.* **2003**, *37*, 4311−4330.
(23) Papageorgiou, S.; Kouvelos, E. P.; Favvas, E.; Sapalidis, A. A.; Romanos, G.; Katsaros, F. Metal−Carboxylate Interactions in Metal−Alginate Complexes Studied with FTIR Spectroscopy. *Carbohydr. Res.* **2010**, *345*, 469−473.
(24) Lee, S.-H.; Park, C.-H. Biosorption of heavy metal ions by brown seaweeds from southern coast of Korea. *Biotechnol. Bioprocess Eng.* **2012**, *17*, 853−861.
(25) Montazer-Rahmati, M. M.; Rabbani, P.; Abdolali, A.; Keshtkar, A. R. Kinetics and equilibrium studies on biosorption of cadmium, lead, and nickel ions from aqueous solutions by intact and chemically modified brown algae. *J. Hazard. Mater.* **2011**, *185*, 401−407.
(26) Papageorgiou, S. K.; Katsaros, F. K.; Kouvelos, E. P.; Nolan, J. W.; Le Deit, H.; Kanellopoulos, N. K. Heavy metal sorption by calcium alginate beads from Laminaria digitata. *J. Hazard. Mater.* **2006**, *137* (3), 1765−1772.
(27) Wang, F.; Lu, X.; Li, X.-y. Selective removals of heavy metals (Pb2+, Cu2+, and Cd2+) from wastewater by gelation with alginate for effective metal recovery. *J. Hazard. Mater.* **2016**, *308*, 75−83.
(28) Park, H. G.; Chae, M. Y. Novel type of alginate gel-based adsorbents for heavy metal removal. *J. Chem. Technol. Biotechnol.* **2004**, *79*, 1080−1083.
(29) Yunxiao, B.; Xiaochang, W. Features and Application of Titanium Dioxide Thin Films in Water Treatment. *Procedia Eng.* **2011**, *24*, 663−666.
(30) Amidon, G. L.; Lee, P.; Topp, E. M. *Transport Processes in Pharmaceutical Systems*; Marcel Dekker: United States, 2000; DOI: 10.1201/9780203909478.
(31) Green, D. W.; Perry, R. H. *Perry's Chemical Engineers' Handbook*, 8th ed.; McGraw-Hill: New York, 2008; Vol. *16*, pp 16−66.
(32) Iulia, N.; Monica, I.; Florea Spiroiu, M.; Ghiurea, M.; Petcu, C.; Cinteza, O. The Adsorption of Heavy Metal Ions on Porous Calcium Alginate Microparticles. *Analele Universitat din Bucuresti-Chimie, Anul XVI (serie noua)* **2007**, 59−67.
(33) Lagoa, R.; Rodrigues, J. Evaluation of Dry Protonated Calcium Alginate Beads for Biosorption Applications and Studies of Lead Uptake. *Appl. Biochem. Biotechnol.* **2007**, *143*, 115−28.
(34) Ho, Y. S.; Ng, J. C. Y.; McKay, G. Kinetics of Pollutant Sorption by Biosorbents: Review. Separation and Purification Methods. *Sep. Purif. Methods* **2000**, *29*, 189−232.
(35) John, A. C.; Ibironke, L. O.; Adedeji; Victor; Oladunni, O. Equilibrium and kinetic studies of the biosorption of heavy metal (cadmium) on Cassia siamea Bark. *Am.-Eurasian J. Sci. Res.* **2011**, *6*, 123−130.
(36) Aluigi, A.; Corbellini, A.; Rombaldoni, F.; Mazzuchetti, G. Wool-derived keratin nanofiber membranes for dynamic adsorption of heavy-metal ions from aqueous solutions. *Text. Res. J.* **2013**, *83*, 1574−1586.
(37) Nastaj, J.; Przewłocka, A.; Rajkowska-Myśliwiec, M. Biosorption of Ni(II), Pb(II) and Zn(II) on calcium alginate beads: equilibrium, kinetic and mechanism studies. *Pol. J. Chem. Technol.* **2016**, *18*, 81.
(38) Fang, Y.; Al-Assaf, S.; Phillips, G. O.; Nishinari, K.; Funami, T.; Williams, P. A. Binding behavior of calcium to polyuronates: Comparison of pectin with alginate. *Carbohydr. Polym.* **2008**, *72* (2), 334−341.
(39) Mohammed, A.; Bissoon, R.; Bajnath, E.; Mohammed, K.; Lee, T.; Bissram, M.; John, N.; Jalsa, N. K.; Lee, K.-Y.; Ward, K. Multistage Extraction and Purification of Waste Sargassum natans to Produce Sodium Alginate: An Optimization Approach. *Carbohydr. Polym.* **2018**, *198*, 109−118.
(40) Murillo-Álvarez, J. I.; Hernández-Carmona, G. Monomer composition and sequence of sodium alginate extracted at pilot plant scale from three commercially important seaweeds from Mexico. *J. Appl. Phycol.* **2007**, *19*, 545−548.
(41) El Atouani, S.; Bentiss, F.; Reani, A.; Zrid, R.; Belattmania, Z.; Pereira, L.; Mortadi, A.; Cherkaoui, O.; Sabour, B. The invasive brown seaweed Sargassum muticum as new resource for alginate in Morocco: Spectroscopic and rheological characterization. *Phycol. Res.* **2016**, *64*, 185−193.
(42) Sulaymon, A. H.; Mohammed, A. A.; Al-Musawi, T. J. Competitive biosorption of lead, cadmium, copper, and arsenic ions using algae. *Environ. Sci. Pollut. Res.* **2013**, *20*, 3011−23.
(43) Barros, M. A. S. D. d.; Gimenes, M. L.; Vieira, M. G. A.; Silva, M. G. C. d. *Ion Exchange Fundamentals and New Challenges, Mass Transfer*; IntechOpen: 2015; DOI: 10.5772/59640.
(44) Pearson, R. G. Hard and Soft Acids and Bases. *J. Am. Chem. Soc.* **1963**, *85*, 3533−3539.
(45) Chen, J. H.; Ni, J. C.; Liu, Q. L.; Li, S. X. Adsorption behavior of Cd(II) ions on humic acid-immobilized sodium alginate and hydroxyl ethyl cellulose blending porous composite membrane adsorbent. *Desalination* **2012**, *285*, 54−61.
(46) Jodra, Y.; Mijangos, F. Ion exchange selectivities of calcium alginate gels for heavy metals. *Water Sci. Technol.* **2001**, *43*, 237−244.
(47) Reddad, Z.; Gérente, C.; Andrès, Y.; Ralet, M.-C.; Thibault, J.-F.; Cloirec, P. L. Ni(II) and Cu(II) binding properties of native and modified sugar beet pulp. *Carbohydr. Polym.* **2002**, *49*, 23−31.
(48) Ho, Y.-S.; McKay, G. Pseudo-Second Order Model for Sorption Process. *Process Biochem.* **1999**, *34*, 451−465.
(49) Madaeni, S. S.; Salehi, E. Membrane-Adsorption Integrated Systems/Processes. *Integr. Membr. Syst. Processes* **2016**, 343−373.
(50) Kafshgari, M. H.; Mansouri, M.; Khorram, M.; Kashani, S. R. Kinetic modeling: a predictive tool for the adsorption of zinc ions onto calcium alginate beads. *Int. J. Ind. Chem.* **2013**, *4*, 5.
(51) Zewail, T. M.; Yousef, N. S. Kinetic study of heavy metal ions removal by ion exchange in batch conical air spouted bed. *Alexandria Eng. J.* **2015**, *54*, 83−90.
(52) Radnia, H. Isotherm and Kinetics of Fe(II) Adsorption onto Chitosan in a Batch Process. *Iran. J. Energy Environ.* **2011**, *2* (3), 250−257.
(53) Enderle, J. D. In *Introduction to Biomedical Engineering*, 3rd ed.; Academic Press: Boston, 2012; DOI: 10.1016/C2009-0-19716-7.
(54) Nai-yu, Z.; Yan-xia, Z.; Xiao, F.; Li-jun, H. Effects of composition and structure of alginates on adsorption of divalent metals. *Chin. J. Oceanol. Limnol.* **1994**, *12*, 78−83.
(55) Ayanda, D. O.; Adeyi, O.; Durojaiye, B.; Olafisoye, O. Adsorption Kinetics and Intraparticulate Diffusivities of Congo Red onto Kola Nut Pod. *Carbon. Polym. J. Environ. Stud.* **2012**, *21* (5), 1147−1152.
(56) Nuhoglu, Y.; Malkoc, E. Thermodynamics and Kinetic Studies for Environment Friendly Ni(II) Biosorption Using Waste Pomace of Olive Oil. *Bioresour. Technol.* **2009**, *100*, 2375−80.
(57) Ramos, P. E.; Silva, P.; Alario, M. M.; Pastrana, L. M.; Teixeira, J. A.; Cerqueira, M. A.; Vicente, A. A. Effect of alginate molecular weight and M/G ratio in beads properties foreseeing the protection of probiotics. *Food Hydrocolloids* **2018**, *77*, 8−16.
(58) Fernández Farrés, I.; Norton, I. T. Formation kinetics and rheology of alginate fluid gels produced by in-situ calcium release. *Food Hydrocolloids* **2014**, *40*, 76−84.

DOI: 10.1021/acs.iecr.8b03691
Ind. Eng. Chem. Res. 2019, 58, 1417−1425